Redox Biology 70 (2024) 103069

Contents lists available at ScienceDirect

Redox Biology

journal homepage: www.elsevier.com/locate/redox

Propagation of a rapid cell-to-cell H_2O_2 signal over long distances in a monolayer of cardiomyocyte cells

Yosef Fichman [a,1], Linda Rowland [b,1], Thi Thao Nguyen [c], Shi-Jie Chen [d], Ron Mittler [b,*]

[a] School of Plant Sciences and Food Security, George S. Wise Faculty of Life Sciences, Tel Aviv University, Tel Aviv, 6997801, Israel
[b] Department of Surgery, University of Missouri School of Medicine, Christopher S. Bond Life Sciences Center, University of Missouri, Columbia, MO, 65201, USA
[c] Gehrke Proteomics Center, Christopher S. Bond Life Sciences Center, University of Missouri, Columbia, MO, 65211, USA
[d] Department of Physics and Astronomy, Department of Biochemistry, Institute of Data Sciences and Informatics, University of Missouri, Columbia, MO 65211-7010, USA

ARTICLE INFO

Keywords:
Cell-to-cell
Gap junction
Hydrogen peroxide
Proteomics
Signal transduction
Superoxide

ABSTRACT

Cell-to-cell communication plays a cardinal role in the biology of multicellular organisms. H_2O_2 is an important cell-to-cell signaling molecule involved in the response of mammalian cells to wounding and other stimuli. We previously identified a signaling pathway that transmits wound-induced cell-to-cell H_2O_2 signals within minutes over long distances, measured in centimeters, in a monolayer of cardiomyocytes. Here we report that this long-distance H_2O_2 signaling pathway is accompanied by enhanced accumulation of cytosolic H_2O_2 and altered redox state in cells along its path. We further show that it requires the production of superoxide, as well as the function of gap junctions, and that it is accompanied by changes in the abundance of hundreds of proteins in cells along its path. Our findings highlight the existence of a unique and rapid long-distance H_2O_2 signaling pathway that could play an important role in different inflammatory responses, wound responses/healing, cardiovascular disease, and/or other conditions.

1. Introduction

Cell-to-cell communication, including paracrine, juxtacrine, and autocrine signaling, plays a cardinal role in the development, maintenance, repair, and milieu/stimuli responses of multicellular organisms. Among the many signals that mediate cell-to-cell signaling, H_2O_2 plays a key role as a regulator of cellular and extracellular redox responses [1–4]. In most cell-to-cell H_2O_2 signaling studies to date, cellular changes in calcium levels, and/or other signals, trigger the production of H_2O_2 by plasma membrane localized dual oxidase (DUOX) and/or NADPH oxidase (NOX)/superoxide dismutases (SODs) [5–13]. Peroxiporins [14,15] can then facilitate the entry of extracellular H_2O_2 into the cells that produced it, or neighboring cells, coordinating their responses to the stimuli [1–4]. H_2O_2-producing complexes/mechanisms packed into exosomes, or proteins secreted by one cell, can also trigger H_2O_2 responses in neighboring cells [16–18]. H_2O_2 signals produced by different cells have multiple functions. For example, in response to wounding, H_2O_2 produced at the injury boundary generates a gradient that attracts leukocytes to the site of injury [19–21]. In other cases, H_2O_2 sensed by neighboring cells via redox-regulated receptors triggers in the receiving cells multiple responses that include changes in calcium levels and the activation kinases [22]. H_2O_2 can also alter the redox state of the producing and receiving cells, and/or the extracellular matrix, and trigger multiple responses [1–4]. It is also possible that peroxiporins facilitate the diffusion of H_2O_2 produced inside the cell by different organelles/compartments contributing to cell-to-cell H_2O_2 signaling [1–4,18,22].

Overall, unless H_2O_2-generating mechanisms are packed into exosomes, it is believed that the distance an extracellular H_2O_2 signal can travel in mammalian tissues is in the range of 100–200 μm, and potentially up to 1 mm[19-21,23]. This limitation is mainly attributed to the H_2O_2 scavenging activity of the extracellular matrix/neighboring cells, that generates a gradient from the producing cells, all the way up to the point H_2O_2 levels drop to normal levels at the tissue(s) they are generated at [19–21,23]. Recent studies in plant and mammalian cells have, however, challenged this concept showing that H_2O_2 signals can propagate within minutes over long distances (measured in centimeters) in different plant tissues, as well as in monolayers of human MDA-MB-231

* Corresponding author.
E-mail address: mittlerr@missouri.edu (R. Mittler).
[1] These authors contributed equally.

https://doi.org/10.1016/j.redox.2024.103069
Received 19 January 2024; Accepted 30 January 2024
Available online 9 February 2024
2213-2317/© 2024 The Authors. Published by Elsevier B.V. This is an open access article under the CC BY-NC-ND license (http://creativecommons.org/licenses/by-nc-nd/4.0/).

breast cancer and rat H9c2 cardiomyocyte cells, and isolated mice hearts [22,24–29]. The mechanism that was proposed to drive this 'long-distance' H_2O_2 signal was termed the reactive oxygen species wave ('ROS wave') and it is based on the enhanced production of H_2O_2 by each cell along the path of the signal. An initiating cell would therefore produce H_2O_2 that is sensed by a neighboring cell and cause it to actively generate H_2O_2, triggering a cascade of cell-to-cell 'enhanced H_2O_2 production' state [22,24–29]. In this respect, it is important to note that it is not H_2O_2 that diffuses over long distances, rather, it is a state of 'enhanced H_2O_2 production' that is propagating in a cell-to-cell fashion from the initiating cell(s) through the tissue, sometimes in a directional manner, with a rate of 0.15–0.4 cm/min [22,24–29]. Although H_2O_2 does not diffuse over long distances *per se* in this cell-to-cell signaling mechanism, it is nonetheless required for the signal to propagate, as external application of catalase, NOX inhibitors, or the introduction of a loss-of-function NOX mutation into cells, block it [22,24–29].

Although the ROS wave has been extensively studied in plants, only one report described it in monolayers of mammalian cells, as well as other eukaryotic organisms such as algae and amoeba (living in a community or film on an agar plate) [24]. Moreover, changes in protein/mRNA expression associated with the ROS wave were only determined in plants and algae [24,25,30]. Many questions regarding this mode of long-distance H_2O_2 signaling in mammalian cells remain, therefore, unanswered. Here, we provide evidence that the long-distance H_2O_2 signal in a monolayer of cardiomyocyte cells is accompanied by changes in protein abundance, enhanced cytosolic H_2O_2 levels, and altered cytosolic redox state, along its path, and that it depends on extracellular production of superoxide, as well as gap junction function.

2. Materials and methods

Cells culture. H9c2 (2–1) rat cardio myoblast (CRL-1446) cells were obtained from ATCC (https://www.atcc.org/) and grown in 37 °C 5% CO_2 RPMI medium 1640 supplemented with 10% FCS, L-glutamine, and antibiotics (ThermoFisher). A day before the experiment the media was replaced with FluoroBrite DMEM (ThermoFisher) to reduce background fluorescence [24,31]. For roGFP2 and roGFP2-Orp1 expressing cells, H9c2 cells were transfected with pMF1707 or pMOS016, obtained from Addgene (https://www.addgene.org/), using the Sigma's gene juice protocol, and selected using a Cytek Aurora cell sorter (Tecan) followed by growth in the presence of the appropriate antibiotics [32–34]. Cells were plated at an initial density of 500,000 per well for the 6-well plate, 25,000 per well for the 96-well plate, and 2,500,000 per dish for the 100 mm dishes and imaged using the IVIS (Revvity) or Lionheart FX (Agilent) apparatuses [24].

IVIS Imaging. Cells were imaged after 2 h of incubation with 20 μM Peroxy Orange 1 (Tocris Bioscience), or 5 μM Dihydroethidium (DHE; Sigma) under the conditions described above [24]. For inhibitor assays, 500U superoxide dismutase (SOD; Sigma), 500U catalase (CAT; Sigma), 50 μM APX115 (MedChemExpress) and/or 50 μM Setanaxib (MedChemExpress), or 600 μM Carbenoxolone (CBX; Sigma) and/or 180 μM and β-glycyrrhetinic acid (βGA; Sigma) were prepared as stock solutions in growth media and diluted (1:1000) into the media culture 1 h before imaging [24]. Injury was performed using an open-flame-heated metal rod (3 mm wide) that touched the local injury area for 1 s as described in Ref. [24]. Untreated, or injured cells, in the presence or absence of inhibitors, were imaged in the same plate/field of view. Images were acquired every 30 s for 30 min. Data analysis was performed with Living Image software using the Math functions. For signal accumulation images, the initial time image was subtracted from all other time images (hence, the absence of signal in the initial image). A signal intensity threshold was implemented based on the untreated field. Total radiant efficiency [24] was quantified by the software in selected regions of interest (ROIs) for local and systemic cells. Statistical analysis was performed as described in Ref. [24]. Briefly, data was obtained from at least 3–5 independent experiments, each including all treatments and controls in the same field of view with 3–5 biological repeats. Data was calculated as percent of 0 min for each treatment and presented in box plots with mean as X ± SE; median is line in the box and box borders are 25th and 75th percentiles; whiskers are the 1.5 interquartile range. Paired Student t-test was conducted using Microsoft Excel (*$P < 0.05$; **$P < 0.01$; ***$P < 0.001$).

For measurements with roGFP2 and roGFP2-Orp1, ratiometric imaging was conducted based on previous studies [28]. RoGFP molecules were excited in two different wave lengths for reduced (490 nm) and oxidized (420 nm) molecules. Fluorescence was collected through emission filter of 520 nm. Ratiometric images were generated using MATLAB (Matworks) using the RatioImage tool where each time point oxidized channel image was divided by the reduced channel image. Data was normalized by "total reduced" cells image (with 1 mM DTT) and "total oxidized" cells image (with 1 mM H_2O_2) [28].

Lionheart FX imaging. Cells were grown as described above and either incubated with 1.25 μM of CellROX orange (ThermoFisher) for 30 min or incubated with 5 μM DHE for 1 h, in the Lionheart FX apparatus under the growth conditions described above. After incubation cells were wounded using an open-flame-heated metal rod (0.5 mm wide) that touched the local injury area for 1 s at one edge of the well. Data was acquired via the Gen5 software (Agilent). Images were acquired simultaneously from the different treatments and controls every 1 min for 2 h. Image analysis was performed with Gen5 and data was exported to Prism 9.4.1 (GraphPad). Experiments were repeated at least 3 times with 3 biological repeats. Line graphs show mean fluorescence in a. u. With S. E. Results were tested for significance with one-way ANOVA.

Protein extraction and proteomics. H9c2 cells were grown as monolayers in 100 mm diameter petri dishes and incubated with DHE or PO1 as described above. The monolayers were then untreated or injured using an open-flame-heated metal rod (3 mm wide) that touched the local injury area for 1 sec[24]. Control and wounded plates were then imaged using the IVIS apparatus for 30 min, as described above, and sampled, based on the imaging results, for proteomics analysis. Cells were scraped from the plates at defined areas (based on signal intensity and location) using cells scrapers (ThermoFisher) in PBS, spun down, immediately resuspended in 1X Laemmli buffer, heated to 95 °C for 10 min, and centrifuged at 16,000 g for 10 min. The supernatant was precipitated with cold acetone. Protein pellets were recovered by centrifugation at 16,000 *g* for 10 min and washed three times with 80% acetone. The final protein pellets were suspended in 6 M urea, 2 M thiourea, and 100 mM ammonium bicarbonate and protein concentration was determined using the Pierce 660 nm Protein Assay (ThermoFisher). Ten micrograms of protein from each sample were then cleaved with trypsin and subjected to proteomics analysis as described in Ref. [24]. The Uniprot ID UP000002494 database was used for protein searching and identification and significant changes (up or down) in protein abundance were determined using unpaired t-tests. Post-analysis based on both MS level and a significance threshold of q-value <0.05, and an absolute average log2 (fold change) > 0.58 were used to identify significant candidates [24]. Proteomics data are available via ProteomeXchange with identifier PXD047131.

Statistical analysis. All experiments were repeated at least three times with at least 3 biological repeats. Box plots graphs are presented with mean as X ± SE; median is line in the box and box borders are 25th and 75th percentiles; whiskers are the 1.5 interquartile range. Paired Student t-test was conducted using Microsoft Excel (*$P < 0.05$; **$P < 0.01$; ***$P < 0.001$).

3. Results and Discussion

The rapid long-distance H_2O_2 signal is accompanied by changes in protein abundance in cells along its path. Monolayers of H9c2 Rat cardiomyocytes cells were injured, imaged, and sampled for proteomics analysis. Cells 0.1–1 cm away from the injury site (termed 'local' cells),

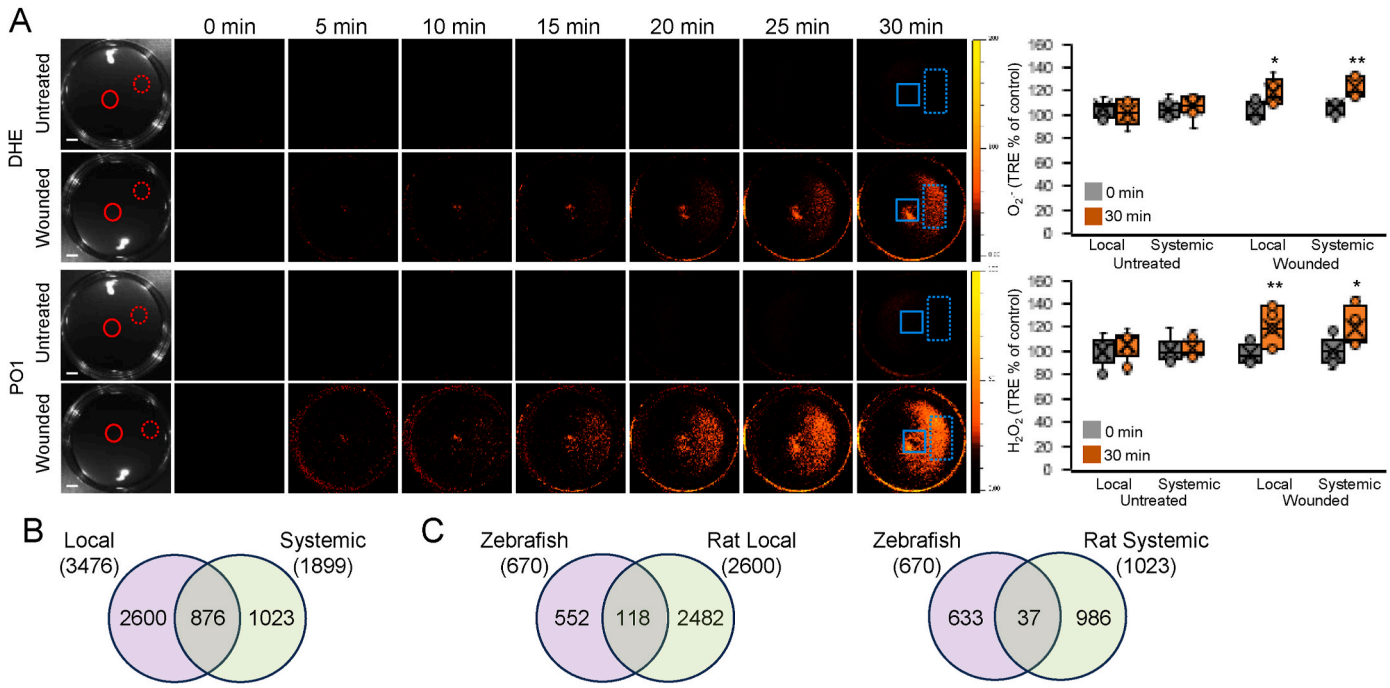

Fig. 1. The wound induced H_2O_2 accumulation signal is accompanied by changes in protein abundance in cells along its path. **A.** Monolayers of rat cardiomyocytes (H9c2) grown in culture were wounded with a heated metal rod to induce injury (average injury diameter is 120 μm) [20] and O_2^- and H_2O_2 accumulation were imaged using DHE and PO1 respectively. Representative time-lapse images of whole plate O_2^- and H_2O_2 accumulation in treated and untreated plates are shown alongside bar graphs of combined data from all plates used for the analysis at the 0- and 30-min time points (local and systemic; Background levels of O_2^- and H_2O_2, measured at time 0, were subtracted from all other time points). Local and systemic sampling locations are indicated with solid and dashed circles, respectively. **B.** Venn diagrams showing changes in protein abundance in local and systemic cells (Following the experimental design shown in A; Local and systemic sampling locations are indicated with solid and dashed rectangles, respectively), 30 min following wounding of the local cells as described above. **C.** Venn diagrams showing overlap between the proteins that changed in abundance in local (Left) or systemic (right) rat cardiomyocytes (B) and proteins that changed in abundance in response to H_2O_2 application in Zebrafish [31]. All experiments were repeated at least 3 times with 10 plates per experiment. Data is presented in A as box plot graphs; X is mean ± S.E., N = 30, $^{**}P < 0.01$, $^{*}P < 0.05$, Student t-test. Scale bar, 2 cm. Abbreviations: DHE, dihydroethdium; PO1, peroxy orange 1; TRE, total radiant efficiency. (For interpretation of the references to colour in this figure legend, the reader is referred to the Web version of this article.)

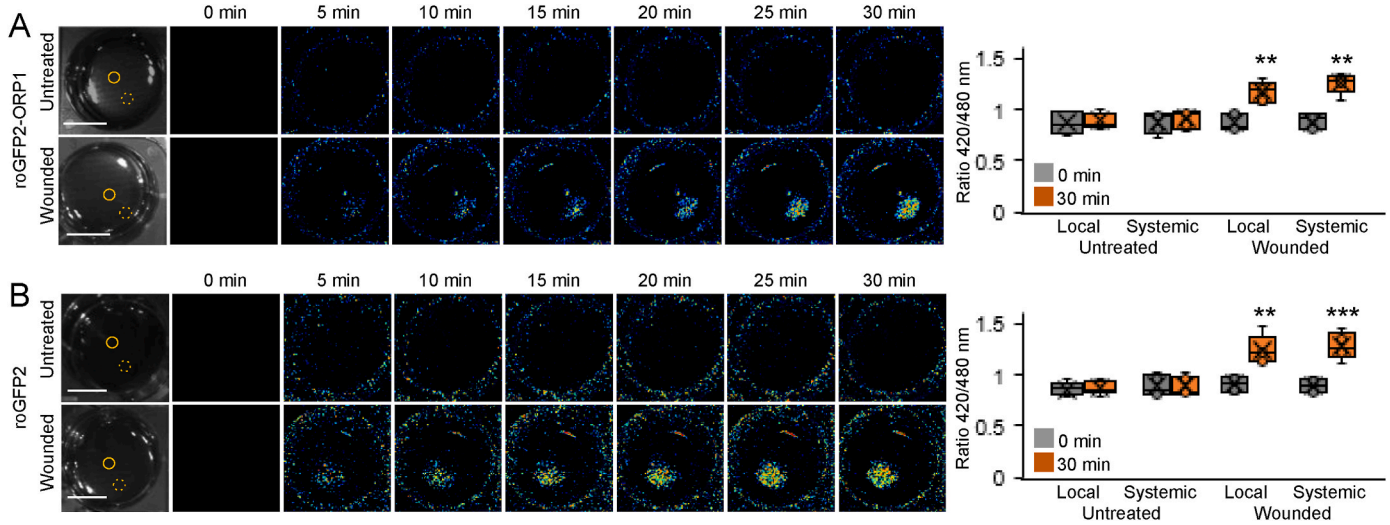

Fig. 2. The wound induced H_2O_2 accumulation signal is accompanied by changes in cytosolic H_2O_2 and redox levels. **A.** Monolayers of rat cardiomyocytes (H9c2) expressing roGFP2-Orp1 grown in culture were wounded with a heated metal rod to induce injury [20] and cytosolic H_2O_2 levels were imaged as the ratio between 420/480 nm [24]. Representative time-lapse images of whole plate changes in cytosolic H_2O_2 levels in treated and untreated plates are shown alongside bar graphs of combined data from all plates used for the analysis at the 0- and 30-min time points (local and systemic; Background levels of cytosolic H_2O_2 levels, measured at time 0, were subtracted from all other time points). **B.** Same as A, but for rat cardiomyocytes (H9c2) expressing roGFP2. Calibration of the roGFP2-Orp1 and roGFP2 signals in rat cardiomyocytes are shown in Fig. S3. All experiments were repeated at least 3 times with 10 plates per experiment. Data is presented in A and B as box plot graphs; X is mean ± S.E., N = 30, $^{**}P < 0.01$, $^{***}P < 0.001$, Student t-test. Scale bar, 1 cm.

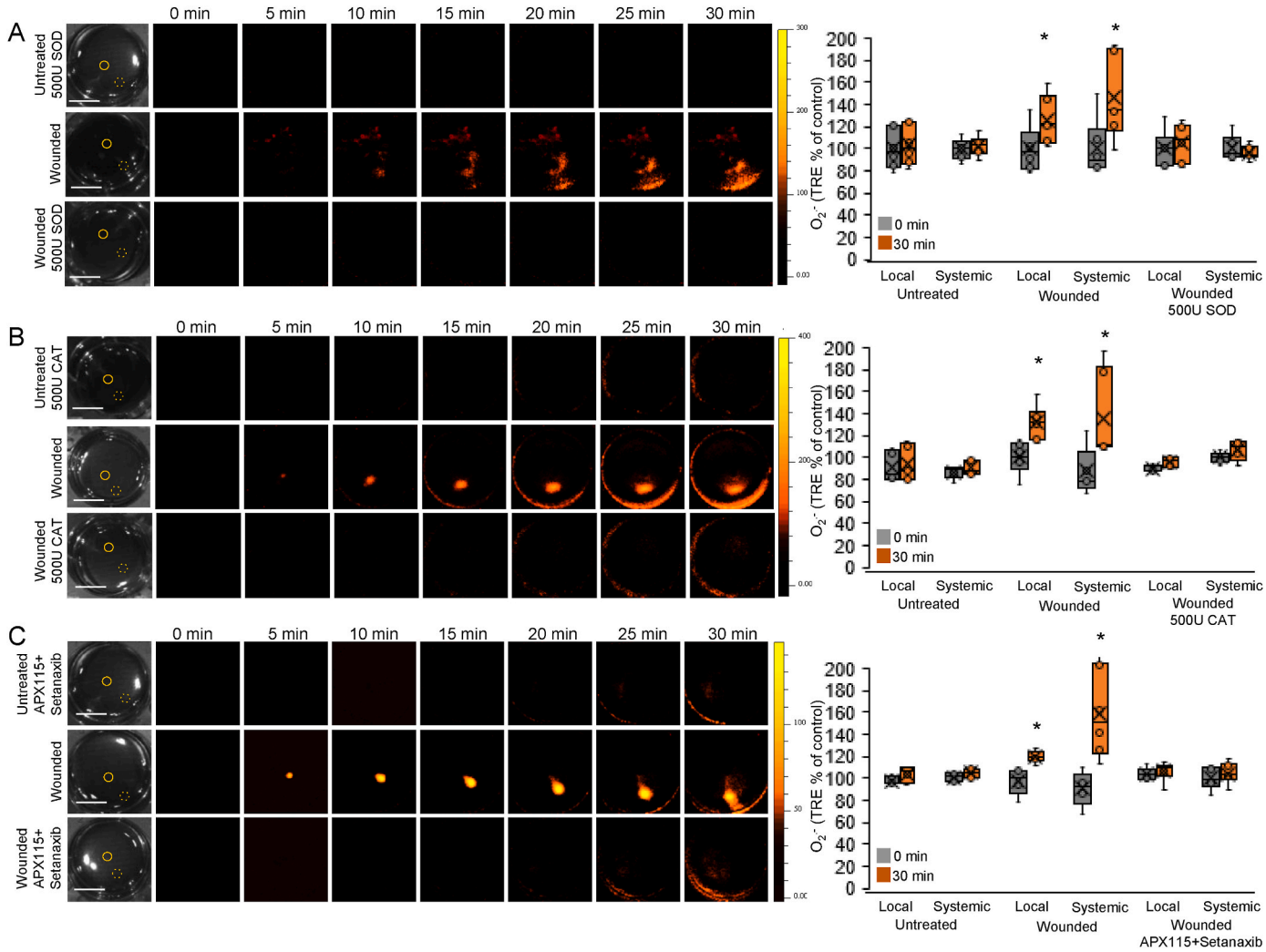

Fig. 3. Inhibition of the wound induced $O_2^{\cdot-}$ accumulation signal with catalase (CAT), superoxide dismutase (SOD), or a mixture of two NADPH oxidase (NOX) inhibitors. **A.** Monolayers of rat cardiomyocytes (H9c2) grown in culture were wounded with a heated metal rod to induce injury [20] and $O_2^{\cdot-}$ accumulation was imaged using DHE in the presence or absence of SOD (added 60 min prior to wounding). Representative time-lapse images of whole plate $O_2^{\cdot-}$ accumulation in treated and untreated plates are shown alongside bar graphs of combined data from all plates used for the analysis at the 0- and 30-min time points (local and systemic; Background levels of $O_2^{\cdot-}$ measured at time 0, were subtracted from all other time points). Local and systemic sampling locations are indicated with solid and dashed circles, respectively. **B.** Same as in A, but instead of SOD, CAT was applied [20]. **C.** Same as in A, but instead of SOD, a mixture of two NOX inhibitors [APX115 (50 μM) and Setanaxib (50 μM)] [20] was applied (application of APX115 or Setanaxib did not inhibit the $O_2^{\cdot-}$ accumulation signal; Fig. S4). All experiments were repeated at least 3 times with 10 plates per experiment. Data is presented in A-C as box plot graphs; X is mean ± S.E., N = 30, *P < 0.05, Student t-test. Scale bar, 1 cm. Abbreviations: CAT, catalase; DHE, dihydroethdium; NOX, NADPH oxidase; SOD, superoxide dismutase; TRE, total radiant efficiency.

as well as cells 3–4 cm away from it (termed 'systemic' cells), were sampled from injured, and uninjured (control) monolayers (Fig. 1A). In parallel, and to confirm that the cells we sampled were producing more ROS, changes in H_2O_2 and $O_2^{\cdot-}$ levels in response to the injury were measured (Fig. 1A). Proteomics analysis of cells sampled from the local and systemic locations of treated and untreated monolayers revealed that, compared to control unwounded cells from these locations, over 3400 and 1800 proteins significantly changed in their abundance in the local and systemic cells within 30 min, in response to wounding, respectively (Fig. 1B–S1; Tables S1–S3). These rapid and statistically significant changes in protein abundance could result from changes in the rate of protein translation, protein degradation, transcription, mRNA processing, or any other changes in the mechanism(s) that control protein steady-state levels in the cells participating in mediating the signal. Importantly, over 870 proteins that changed in abundance in local cells also changed in abundance in systemic cells (Fig. 1B; Table S3). These proteins could be directly associated with the 'enhanced H_2O_2 production state' triggered in the local and systemic cells in response to wounding (Fig. 1A). This group of proteins was enriched in molecular chaperone, oxidoreductase acting on sulfur, and membrane insertase activities (Fig. S1C), and included proteins such as ferredoxin, thioredoxin, MnSOD, catalase, peroxiredoxin, ferritin, and different proteins involved in glutathione metabolism (Table S3), suggesting that they are associated with altered redox/H_2O_2 levels in cells. An overlap between the proteins identified in response to wounding by our study and zebrafish proteins altered in response to H_2O_2 was also found (Fig. 3C) [35].

In addition to imaging H_2O_2 levels with the IVIS apparatus (Fig. 1A), we also used an automated fluorescent microscope to measure the rates of ROS accumulation in cells along the path of the signal (Fig. S2). This analysis revealed that the highest rates of ROS accumulation occurred close to the injury site, followed by lower rates at the middle and opposite edge of the long-distance H_2O_2 signal path (Fig. S2). This analysis further supported the model of enhanced H_2O_2 production by different cells along the path of the signal [4,24,25]. The identified proteins/pathways associated with the state of enhanced H_2O_2

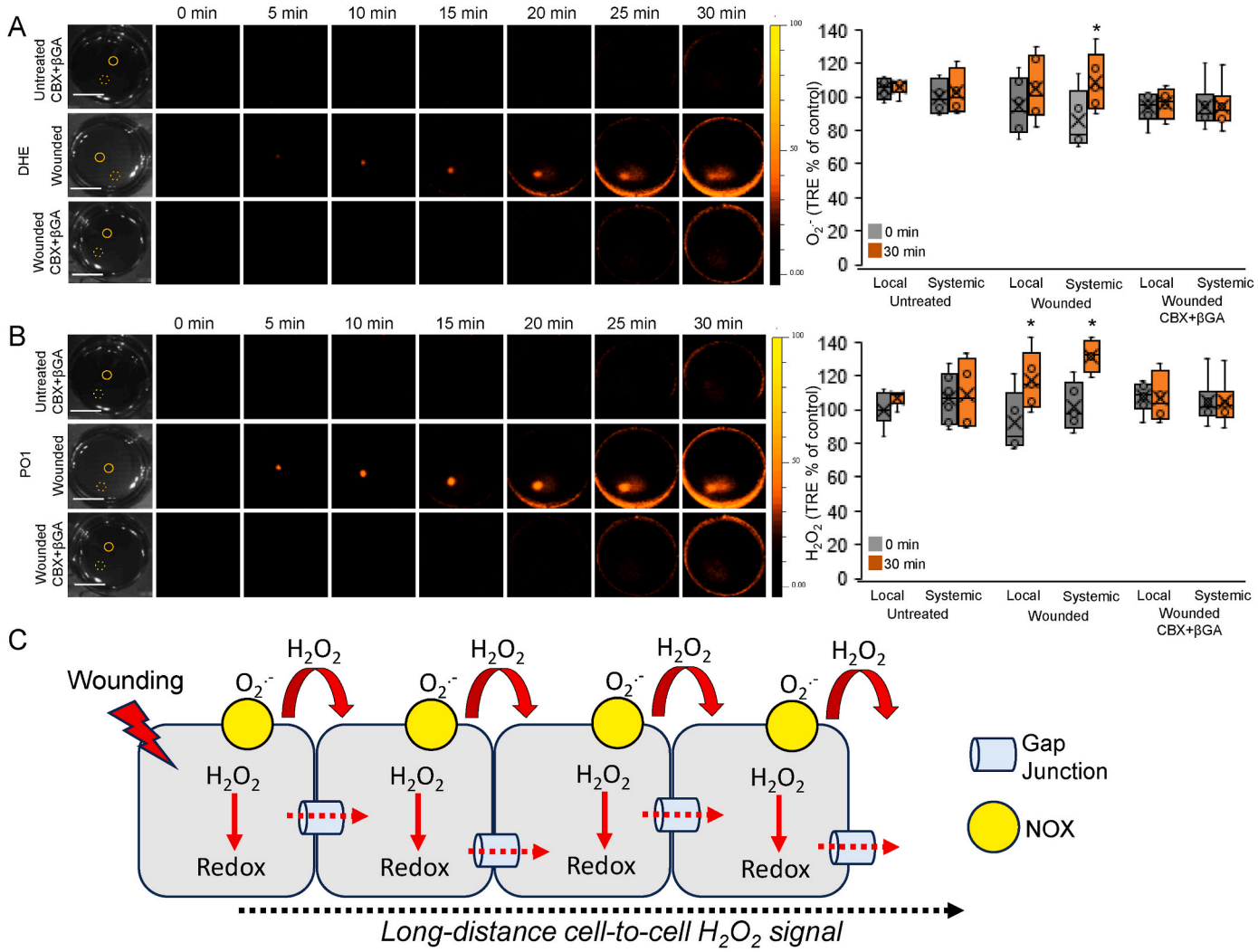

Fig. 4. Inhibition of the wound induced H_2O_2 and $O_2^{\cdot-}$ accumulation signal with gap junction inhibitors, and a model. **A.** Monolayers of rat cardiomyocytes (H9c2) grown in culture were wounded with a heated metal rod to induce injury [20] and $O_2^{\cdot-}$ accumulation was imaged using DHE in the presence or absence of a mixture of Carbenoxolone (CBX; 600 μM) and β-glycyrrhetinic acid (βGA; 180 μM), added 60 min prior to wounding. Representative time-lapse images of whole plate $O_2^{\cdot-}$ accumulation in treated and untreated plates are shown alongside bar graphs of combined data from all plates used for the analysis at the 0- and 30-min time points (local and systemic; Background levels of $O_2^{\cdot-}$ measured at time 0, were subtracted from all other time points). Local and systemic sampling locations are indicated with solid and dashed circles, respectively. **B.** Same as in A, but instead of DHE, PO1 (H_2O_2 accumulation) was used for imaging. **C.** A hypothetical model of the wound induced H_2O_2 and $O_2^{\cdot-}$ accumulation cell-to-cell signal. Each sell along the path of the signal is shown to produce H_2O_2 and $O_2^{\cdot-}$ propagating the signal across long distances in a process that requires NOX and gap junction function (*i.e.,* a mixture of paracrine and juxtacrine signaling). See text for more details. All experiments were repeated at least 3 times with 10 plates per experiment. Data is presented in A and B as box plot graphs; X is mean ± S.E., N = 30, *P < 0.05, Student t-test. Scale bar, 1 cm. Abbreviations: βGA, β-glycyrrhetinic acid; CBX, Carbenoxolone; DHE, dihydroethdium; NOX, NADPH oxidase; PO1, peroxy orange 1; TRE, total radiant efficiency. (For interpretation of the references to colour in this figure legend, the reader is referred to the Web version of this article.)

production (Fig. 1, S1; Tables S1–S3) could be used in future studies to dissect the process of long-distance cell-to-cell H_2O_2 signaling, especially since some of them were not previously associated with responses to H_2O_2/ROS (Fig. 1C; Tables S1–S3). Although it would be ideal to study the proteomics responses of H9c2 monolayers treated with an external antioxidant, or composed of NOX/DOUX mutants, these treatments/manipulations would affect both the initiation as well as the propagation of the H_2O_2 signal and would not provide a high-resolution analysis of this process. Instead, methods to generate or print monolayers composed of sections that contain NOX/DOUX mutations flanked by sections that do not (like our studies in *Chlamydomonas*) [24] should be developed. Single-cell proteomics and/or transcriptomics studies should also be conducted in future studies, as they may uncover additional proteins and transcripts involved in this process.

Enhanced cytosolic accumulation of H_2O_2 and changes in the redox sate of cells along the path of the H_2O_2 signal. We previously imaged the long-distance H_2O_2 signal in different organisms using various H_2O_2/ROS-sensitive dyes [24]. These methods could however complicate the interpretation of results [2]. In addition, they did not measure changes in redox levels associated with the signal. We, therefore, generated monolayers of H9c2 rat cardiomyocyte cells expressing cytosolic roGFP2 (for redox), or cytosolic roGFP2-Orp1 (for H_2O_2), imaging (Fig. 2, S3). Analysis of wounded and unwounded H9c2 monolayers expressing these proteins revealed that the long-distance H_2O_2 signal is accompanied by enhanced cytosolic accumulation of H_2O_2 as well as changes in the redox state of cells along its path. These findings provide direct evidence for the putative function of the signal in altering the redox state of cells along its path, thereby, activating different redox responses (also supported by the identification of redox-response proteins in our proteomics analysis; Table S3).

Production of extracellular superoxide and gap junction function are required for the propagation of the long-distance H_2O_2 signal.

H_2O_2-mediated cell-to-cell signaling in monolayers of H9c2 cells was previously shown to be blocked by catalase application, as well as a mixture of the NOX inhibitors APX115 and Setanaxib (but not each of these inhibitors applied individually; suggesting that NOX1 or NOX2, and NOX4 might be involved in mediating this process) [24]. However, the role of superoxide in this signaling pathway was not substantiated. We therefore used external application of SOD, as well as imaging using DHE in our experimental system. As shown in Fig. 1A and 3A, 3B we could image the progression of the signal using DHE, and this signal was blocked by SOD or catalase application. In addition, a mixture of two NOX inhibitors blocked the signal imaged with DHE (Fig. 3B–S4). These findings are highly intriguing, as they support a model in which both superoxide and H_2O_2 are essential for the propagation of the long-distance H_2O_2 signal. Adding excess SOD, that should have simply converted superoxide to H_2O_2 and supported the signal, was therefore found to, instead, block it (Fig. 3A). This could suggest that a minimal/threshold level of superoxide produced extracellularly is needed for the signal to propagate, and that superoxide could function in other, yet unknown, ways as a signal required for this pathway (as opposed to simply being a substrate for SODs to generate H_2O_2). Further studies are needed to address this intriguing possibility.

The 'ROS wave' long-distance H_2O_2 signal of plants was shown to require paracrine as well as juxtacrine signaling (the latter requiring the function of plasmodesmata, the plant equivalents of gap junctions) [22, 24–30]. As cardiomyocytes contain multiple types of gap junctions, including some that may be used to secrete compounds from the cell to the extracellular matrix upon wounding [36,37], we tested the impact of different gap junction inhibitors on the cell-to-cell H_2O_2 signal. To test whether gap junction function is required for the long-distance H_2O_2 signal in H9c2 cells, we treated monolayers of H9c2 cells with CBX [38], βGA [39], or a mixture of the two [40], prior to wounding. The combination of CBX+βGA, but not CBX or βGA (potentially due to the presence of multiple gap junction types in cardiomyocytes) blocked the progression of the H_2O_2 signal, imaged with DHE or PO1 (Fig. 4, S5). Our findings (Figs. 2 and 4) [24] support, therefore, a model in which paracrine and juxtacrine signaling, are both required for the propagation of the long-distance H_2O_2 pathway in mammalian cells (Fig. 4C). They further provide a potential mechanistic explanation to the directionality of the signal in H9c2 cells. While in other eukaryotic organisms, such as *Chlamydomonas* cells (that lacks gap junction) or MDA-MB-231 cells (growing as a monolayer with poor gap junction connectivity), the signal appears to diffuse away from the site of injury, without a clear direction, in H9c2 cells (that are highly connected to each other via multiple gap junctions), it appears to be directional, following the orientation of cells in the monolayer [24]. This directionality could be related to the many different gap junctions that connect H9c2 cells and direct the signal along a specific path [36,37]. In future studies, the polarity, and other aspects of the directionality of the signal, should be addressed, as these could play a key role in the function of the H_2O_2 signal in different tissues. As gap junctions are involved in mediating the long-distance cell-to-cell H_2O_2 signal (Fig. 4, S5), it is also possible that H_2O_2 produced inside the cell (*e.g.,* by NOX 4 at the mitochondria) [41] participates in this pathway.

Summary and conclusions. Taken together, our findings reveal that the long-distance H_2O_2 cell-to-cell signaling pathway triggered by wounding in a monolayer of H9c2 cells (Fig. 4C) is accompanied by enhanced accumulation of H_2O_2 and altered redox state at the cytosol of cells along its path, as well as significant changes in the abundance of hundreds of proteins. In addition, we show that this pathway requires the production of superoxide as well as the function of gap junctions. As H_2O_2 signaling plays such a key role in mammalian physiology and development [1–3], more studies are needed to dissect this pathway and determine how it is involved in different inflammatory responses, wound healing, development, cardiovascular disease, and other diseases/conditions.

Funding

This work was supported by funding from the National Science Foundation (IOS-1932639, MCB2224839), and the National Institute of Health grant (GM111364, R35GM134919).

Use of AI and AI-assisted technologies-

None.

CRediT authorship contribution statement

Yosef Fichman: Data curation, Formal analysis, Investigation, Methodology, Writing – review & editing. **Linda Rowland:** Data curation, Formal analysis, Methodology. **Thi Thao Nguyen:** Data curation, Formal analysis, Methodology. **Shi-Jie Chen:** Conceptualization, Writing – review & editing. **Ron Mittler:** Conceptualization, Funding acquisition, Investigation, Resources, Writing – original draft, Writing – review & editing.

Declaration of competing interest

The authors declare that they have no known competing financial interests or personal relationships that could have appeared to influence the work reported in this paper.

Acknowledgments

pMF1707 was a gift from Dr. Marc Fransen (Addgene plasmid 125584) and pMOS016 was a gift from Dr. Adam Cohen (Addgene plasmid 163058).

Appendix A. Supplementary data

Supplementary data to this article can be found online at https://doi.org/10.1016/j.redox.2024.103069.

References

[1] H. Sies, D.P. Jones, Reactive oxygen species (ROS) as pleiotropic physiological signalling agents, Nat. Rev. Mol. Cell Biol. 21 (7) (2020 Jul) 363–383, https://doi.org/10.1038/s41580-020-0230-3.
[2] H. Sies, V.V. Belousov, N.S. Chandel, M.J. Davies, D.P. Jones, G.E. Mann, M. P. Murphy, M. Yamamoto, C. Winterbourn, Defining roles of specific reactive oxygen species (ROS) in cell biology and physiology, Nat. Rev. Mol. Cell Biol. 23 (7) (2022 Jul) 499–515, https://doi.org/10.1038/s41580-022-00456-z.
[3] H. Sies, Hydrogen peroxide as a central redox signaling molecule in physiological oxidative stress: oxidative eustress, Redox Biol. 11 (2017 Apr) 613–619, https://doi.org/10.1016/j.redox.2016.12.035.
[4] R. Mittler, S.I. Zandalinas, Y. Fichman, F. Van Breusegem, Reactive oxygen species signalling in plant stress responses, Nat. Rev. Mol. Cell Biol. 23 (10) (2022 Oct) 663–679, https://doi.org/10.1038/s41580-022-00499-2.
[5] A. Pató, K. Bölcskei, Á. Donkó, D. Kaszás, M. Boros, L. Bodrogi, G. Várady, V.F. S. Pape, B.T. Roux, B. Enyedi, Z. Helyes, F.M. Watt, G. Sirokmány, M. Geiszt, Hydrogen peroxide production by epidermal dual oxidase 1 regulates nociceptive sensory signals, Redox Biol. 62 (2023 Jun) 102670, https://doi.org/10.1016/j.redox.2023.102670.
[6] B. Enyedi, M. Zana, Á. Donkó, M. Geiszt, Spatial and temporal analysis of NADPH oxidase-generated hydrogen peroxide signals by novel fluorescent reporter proteins, Antioxidants Redox Signal. 19 (6) (2013 Aug 20) 523–534, https://doi.org/10.1089/ars.2012.4594.
[7] M.J. Grubisha, M.E. Cifuentes, S.R. Hammes, D.B. Defranco, A local paracrine and endocrine network involving TGFβ, Cox-2, ROS, and estrogen receptor β influences reactive stromal cell regulation of prostate cancer cell motility, Mol. Endocrinol. 26 (6) (2012 Jun) 940–954, https://doi.org/10.1210/me.2011-1371.
[8] M. Xu, Y. Zhang, M. Xia, X.X. Li, J.K. Ritter, F. Zhang, P.L. Li, NAD(P)H oxidase-dependent intracellular and extracellular $O_2^{\bullet-}$ production in coronary arterial myocytes from CD38 knockout mice, Free Radic. Biol. Med. 52 (2) (2012 Jan 15) 357–365, https://doi.org/10.1016/j.freeradbiomed.2011.10.485.
[9] G. Csányi, W.R. Taylor, P.J. Pagano, NOX and inflammation in the vascular adventitia, Free Radic. Biol. Med. 47 (9) (2009 Nov 1) 1254–1266, https://doi.org/10.1016/j.freeradbiomed.2009.07.022.
[10] A. Cadiz Diaz, N.A. Schmidt, M. Yamazaki, C.J. Hsieh, T.S. Lisse, S. Rieger, Coordinated NADPH oxidase/hydrogen peroxide functions regulate cutaneous

sensory axon de- and regeneration, Proc. Natl. Acad. Sci. U. S. A. 119 (30) (2022 Jul 26) e2115009119, https://doi.org/10.1073/pnas.2115009119.
[11] I.R. Evans, F.S. Rodrigues, E.L. Armitage, W. Wood, Draper/CED-1 mediates an ancient damage response to control inflammatory blood cell migration in vivo, Curr. Biol. 25 (12) (2015 Jun 15) 1606–1612, https://doi.org/10.1016/j.cub.2015.04.037.
[12] J.P. Taylor, H.M. Tse, The role of NADPH oxidases in infectious and inflammatory diseases, Redox Biol. 48 (2021 Dec) 102159, https://doi.org/10.1016/j.redox.2021.102159.
[13] J.L. Meitzler, Purification and characterization of DUOX peroxidase homology domains (PHDs), Methods Mol. Biol. 1982 (2019) 61–74, https://doi.org/10.1007/978-1-4939-9424-3_4.
[14] M.N. Möller, E. Cuevasanta, F. Orrico, A.C. Lopez, L. Thomson, A. Denicola, Diffusion and transport of reactive species across cell membranes, Adv. Exp. Med. Biol. 1127 (2019) 3–19, https://doi.org/10.1007/978-3-030-11488-6_1.
[15] G.P. Bienert, F. Chaumont, Aquaporin-facilitated transmembrane diffusion of hydrogen peroxide, Biochim. Biophys. Acta 1840 (5) (2014 May) 1596–1604, https://doi.org/10.1016/j.bbagen.2013.09.017.
[16] S.V. Petersen, N.B. Poulsen, C. Linneberg Matthiesen, F. Vilhardt, Novel and converging ways of NOX2 and SOD3 in trafficking and redox signaling in macrophages, Antioxidants 10 (2) (2021 Jan 25) 172, https://doi.org/10.3390/antiox10020172.Vesicles.
[17] I. Amblard, M. Thauvin, C. Rampon, I. Queguiner, V.V. Pak, V. Belousov, A. Prochiantz, M. Volovitch, A. Joliot, S. Vriz, H_2O_2 and Engrailed 2 paracrine activity synergize to shape the zebrafish optic tectum, Commun. Biol. 3 (1) (2020 Sep 29) 536, https://doi.org/10.1038/s42003-020-01268-7.
[18] T. Buck, C.T. Hack, D. Berg, U. Berg, L. Kunz, A. Mayerhofer, The NADPH oxidase 4 is a major source of hydrogen peroxide in human granulosa-lutein and granulosa tumor cells, Sci. Rep. 9 (1) (2019 Mar 5) 3585, https://doi.org/10.1038/s41598-019-40329-8.
[19] P. Niethammer, C. Grabher, A.T. Look, T.J. Mitchison, A tissue-scale gradient of hydrogen peroxide mediates rapid wound detection in zebrafish, Nature 459 (7249) (2009 Jun 18) 996–999, https://doi.org/10.1038/nature08119.
[20] W. Razzell, I.R. Evans, P. Martin, W. Wood, Calcium flashes orchestrate the wound inflammatory response through DUOX activation and hydrogen peroxide release, Curr. Biol. 23 (5) (2013 Mar 4) 424–429, https://doi.org/10.1016/j.cub.2013.01.058.
[21] A. Katikaneni, M. Jelcic, G.F. Gerlach, Y. Ma, M. Overholtzer, P. Niethammer, Lipid peroxidation regulates long-range wound detection through 5-lipoxygenase in zebrafish, Nat. Cell Biol. 22 (9) (2020 Sep) 1049–1055, https://doi.org/10.1038/s41556-020-0564-2.
[22] Y. Fichman, S.I. Zandalinas, S. Peck, S. Luan, R. Mittler, HPCA1 is required for systemic reactive oxygen species and calcium cell-to-cell signaling and plant acclimation to stress, Plant Cell 34 (11) (2022 Oct 27) 4453–4471, https://doi.org/10.1093/plcell/koac241.
[23] T. Sousa, M. Gouveia, R.D.M. Travasso, A. Salvador, How abundant are superoxide and hydrogen peroxide in the vasculature lumen, how far can they reach? Redox Biol. 58 (2022 Dec) 102527 https://doi.org/10.1016/j.redox.2022.102527.
[24] Y. Fichman, L. Rowland, M.J. Oliver, R. Mittler, ROS are evolutionary conserved cell-to-cell stress signals, Proc. Natl. Acad. Sci. U. S. A. 120 (31) (2023 Aug) e2305496120, https://doi.org/10.1073/pnas.2305496120.
[25] M.Á. Peláez-Vico, Y. Fichman, S.I. Zandalinas, F. Van Breusegem, S.M. Karpiński, R. Mittler, ROS and redox regulation of cell-to-cell and systemic signaling in plants during stress, Free Radic. Biol. Med. 193 (Pt 1) (2022 Nov 20) 354–362, https://doi.org/10.1016/j.freeradbiomed.2022.10.305.
[26] S.I. Zandalinas, Y. Fichman, R. Mittler, Vascular bundles mediate systemic reactive oxygen signaling during light stress, Plant Cell 32 (11) (2020 Nov) 3425–3435, https://doi.org/10.1105/tpc.20.00453.
[27] Y. Fichman, R.J. Myers Jr., D.G. Grant, R. Mittler, Plasmodesmata-localized proteins and ROS orchestrate light-induced rapid systemic signaling in *Arabidopsis*, Sci. Signal. 14 (671) (2021 Feb 23) eabf0322, https://doi.org/10.1126/scisignal.abf0322.
[28] Y. Fichman, R. Mittler, A systemic whole-plant change in redox levels accompanies the rapid systemic response to wounding, Plant Physiol 186 (1) (2021 May 27) 4–8, https://doi.org/10.1093/plphys/kiab022.
[29] G. Miller, K. Schlauch, R. Tam, D. Cortes, M.A. Torres, V. Shulaev, J.L. Dangl, R. Mittler, The plant NADPH oxidase RBOHD mediates rapid systemic signaling in response to diverse stimuli, Sci. Signal. 2 (84) (2009 Aug 18) ra45, https://doi.org/10.1126/scisignal.2000448.
[30] S.I. Zandalinas, Y. Fichman, A.R. Devireddy, S. Sengupta, R.K. Azad, R. Mittler, Systemic signaling during abiotic stress combination in plants, Proc. Natl. Acad. Sci. U. S. A. 117 (24) (2020 Jun 16) 13810–13820, https://doi.org/10.1073/pnas.2005077117.
[31] L. Rowland, H.B. Marjault, O. Karmi, D. Grant, L.J. Webb, A. Friedler, R. Nechushtai, R. Elber, R. Mittler, A combination of a cell penetrating peptide and a protein translation inhibitor kills metastatic breast cancer cells, Cell Death Discov 9 (1) (2023 Aug 31) 325, https://doi.org/10.1038/s41420-023-01627-3.
[32] O. Karmi, Y.S. Sohn, S.I. Zandalinas, L. Rowland, S.D. King, R. Nechushtai, R. Mittler, Disrupting CISD2 function in cancer cells primarily impacts mitochondrial labile iron levels and triggers TXNIP expression, Free Radic. Biol. Med. 176 (2021 Nov 20) 92–104, https://doi.org/10.1016/j.freeradbiomed.2021.09.013. Transfection, proteomics.
[33] O. Karmi, L. Rowland, S.D. King, C. Manrique-Acevedo, I.Z. Cabantchik, R. Nechushtai, R. Mittler, The [2Fe-2S] protein CISD2 plays a key role in preventing iron accumulation in cardiomyocytes, FEBS Lett. 596 (6) (2022 Mar) 747–761, https://doi.org/10.1002/1873-3468.14277. Proteomics.
[34] Y.S. Sohn, S. Tamir, L. Song, D. Michaeli, I. Matouk, A.R. Conlan, Y. Harir, S. H. Holt, V. Shulaev, M.L. Paddock, A. Hochberg, I.Z. Cabanchick, J.N. Onuchic, P. A. Jennings, R. Nechushtai, R. Mittler, NAF-1 and mitoNEET are central to human breast cancer proliferation by maintaining mitochondrial homeostasis and promoting tumor growth, Proc. Natl. Acad. Sci. U. S. A. 110 (36) (2013 Sep 3) 14676–14681, https://doi.org/10.1073/pnas.1313198110. DHE imaging.
[35] T.S. Lisse, B.L. King, S. Rieger, Comparative transcriptomic profiling of hydrogen peroxide signaling networks in zebrafish and human keratinocytes: implications toward conservation, migration and wound healing, Sci. Rep. 6 (2016 Feb 5) 20328, https://doi.org/10.1038/srep20328.
[36] T. Martins-Marques, Connecting different heart diseases through intercellular communication, Biol Open 10 (9) (2021 Sep 15) bio058777, https://doi.org/10.1242/bio.058777.
[37] R.D. Johnson, P. Camelliti, Role of non-myocyte gap junctions and connexin hemichannels in cardiovascular Health and disease: novel therapeutic targets? Int. J. Mol. Sci. 19 (3) (2018 Mar 15) 866, https://doi.org/10.3390/ijms19030866.
[38] Z.J. Du, G.Q. Cui, J. Zhang, X.M. Liu, Z.H. Zhang, Q. Jia, J.C. Ng, C. Peng, C.X. Bo, H. Shao, Inhibition of gap junction intercellular communication is involved in silica nanoparticles-induced H9c2 cardiomyocytes apoptosis via the mitochondrial pathway, Int J Nanomedicine 12 (2017 Mar 20) 2179–2188, https://doi.org/10.2147/IJN.S127904.
[39] M. Zaniboni, A. Rossini, P. Swietach, N. Banger, K.W. Spitzer, R.D. Vaughan-Jones, Proton permeation through the myocardial gap junction, Circ. Res. 93 (8) (2003 Oct 17) 726–735, https://doi.org/10.1161/01.RES.0000093986.47383.CE.
[40] E.J. Behringer, M.J. Socha, L. Polo-Parada, S.S. Segal, Electrical conduction along endothelial cell tubes from mouse feed arteries: confounding actions of glycyrrhetinic acid derivatives, Br. J. Pharmacol. 166 (2) (2012 May) 774–787, https://doi.org/10.1111/j.1476-5381.2011.01814.x.
[41] D. Wang, J. Li, G. Luo, J. Zhou, N. Wang, S. Wang, R. Zhao, X. Cao, Y. Ma, G. Liu, L. Hao, Nox4 as a novel therapeutic target for diabetic vascular complications, Redox Biol. 64 (2023 Aug) 102781, https://doi.org/10.1016/j.redox.2023.102781.